

# We are IntechOpen, the world's leading publisher of Open Access books Built by scientists, for scientists

6,900

Open access books available

185,000

International authors and editors

200M

Downloads

Our authors are among the

154

Countries delivered to

TOP 1%

most cited scientists

12.2%

Contributors from top 500 universities



WEB OF SCIENCE™

Selection of our books indexed in the Book Citation Index  
in Web of Science™ Core Collection (BKCI)

Interested in publishing with us?  
Contact [book.department@intechopen.com](mailto:book.department@intechopen.com)

Numbers displayed above are based on latest data collected.  
For more information visit [www.intechopen.com](http://www.intechopen.com)



# Investigation of Strain Effect on Cleavage Fracture for Reactor Pressure Vessel Material

*Kushal Bhattacharyya*

## Abstract

Failure mechanism of 20MnMoNi55 steel in the lower self of ductile to brittle transition (DBT) region is considered as brittle fracture but it has been observed from the experimental analysis of stress-strain diagram that clear plastic deformation is shown by the material before failure. Therefore, strain correction is implemented in the cleavage fracture model proposed by different researchers in the lower self of the DBT region with the help of finite element analysis. To avoid a huge number of experiments being performed, Monte Carlo simulation is used to generate a huge number of random data at different temperatures in the lower self of the DBT region for calibration of the cleavage parameters with the help of the master curve methodology. Fracture toughness calculated after strain correction through different models are validated with experimental results for the different probability of failures.

**Keywords:** fracture toughness, plastic strain, reactor pressure vessel, master curve, finite element analysis

## 1. Introduction

Regular maintenance of the reactor pressure vessel (RPV) is an important criterion that has to be considered where safety is the prime requirement for any country. In that respect embrittlement of the RPV material has to be quantified concerning reference temperature  $T_0$ . In the last few decades, several researchers tried to quantify this embrittlement nature of ferritic steel in RPV materials. Among them, the work done by Kim Wallin with the development of ASTM E1921 and master curve [1–3] proved to be quite impressive and acceptable in quantifying embrittlement for different ferritic steels used in reactor pressure vessels with the help of reference temperature  $T_0$ .

It has been observed in our previous work that references temperature ( $T_0$ ) predicted for 20MnMoNi55 steel is constraint dependent [4] and it varies with different crack length, thickness, and geometry of the specimen. It also shows the variation with test temperature and censor parameter “m”.

This observation is also predicted by different researchers [5–10] working in this field of ductile to brittle transition (DBT) region for different RPV materials.

Therefore, in the last few years, the main aim of the researchers was focused to study the constraint effects of reference temperature  $T_0$  for RPV materials. Finite element analysis is considered a useful tool to study the stress distribution near the crack tip of the specimen at different temperatures in the DBT region. With this aim in mind some researchers try to capture the constraint effect with the help of T-stress [11–15], Q-stress [16–18] and triaxiality [19]. The author also tried to capture the loss of constraint effect on the reference temperature  $T_0$  for these RPV materials with the help of these three stress-based parameters in his earlier work [20]. A satisfactory correlation of the constraint effect in the upper domain of the ductile failure-dominated region of the DBT region is observed. But the brittle failure-dominated region or the lower transition region remains untouched. Therefore, many researchers tried to address the lower transition region with different cleavage failure models. Among them, the work is done by Beremin [21] and his co-authors prove to be challenging for the RPV materials at the brittle failure-dominated portion of the DBT region. The author is motivated to explore a brittle failure model to capture the constraint effect satisfactorily in the lower transition region. With that framework in mind, the widely accepted Beremin model [21] is used to study the constraint effect on master curve and reference temperature ( $T_0$ ) by different researchers for 20 years or more. Beremin cleavage fracture model provides a good correlation between localized stress pattern prevailing near the crack tip with that of global parameters of fracture like J-integral, applied to load, and fracture toughness with the help of Weibull stress a parameter of stress as coined by Beremin. But the calibration of the constant parameters which remain unique for the material is a challenging job because it demands to test more than 30 specimens to predict a reliable result as predicted by Khalili and Kromp [22]. But testing such a huge number of tests for a given material and at a given test temperature is much expensive. Therefore, many authors utilized the Monta Carlo simulation to generate a huge random number of data from the 6 experimental fracture toughness results to determine the parameters at different temperatures. The entire process is explained in the author's previous work [23].

Beremin model is entirely focused on brittle fracture where no strained effect is considered but it has been observed in the experimental stress-strain diagram for the material 20MnMoNi55 steel a huge plastic deformation is observed in the material before failure even at  $-110^\circ\text{C}$  and the plastic region diminishes as it moves towards  $-150^\circ\text{C}$ . Therefore, strain correction is required in the model for proper calibration of the Beremin parameters for the material. Beremin himself in his work felt the requirement for strain correction and he simultaneously developed a model considering the effect of strain in calculating Weibull Stress [21]. Recently, Ruggieri in his work [24, 25] utilized the strain effect by different models for a similar type of RPV material A515 Gr 65 pressure vessel steel. But he uses the toughness scaling model to calibrate the Beremin model parameters.

In December 2017, Claudio Ruggieri, Robert H. Dodds Jr. [26] through their work focuses on the importance of plastic strain effects into the probabilistic framework in brittle fracture.

In November 2019, Claudio Ruggieri [27] through his work proposed a probabilistic, micromechanics-based model which incorporates plastic strain effects on cleavage fracture and its dependence on the microcrack distribution. The model utilized a plastic-strain based form of the Weibull stress to capture the differences in brittle fracture toughness for a reactor pressure vessel (RPV) steel due to constraint loss.

In the present work fracture toughness of 20MnMoNi55 steel is determined with the help of three-point bending (TPB) at  $-100^\circ\text{C}$ ,  $-110^\circ\text{C}$ ,  $-120^\circ\text{C}$ ,  $-130^\circ\text{C}$ ,

-140°C, at reference temperature  $T_0$  and master curve is calculated for all of this results. Then elastoplastic finite element analysis of each fracture specimen is performed taking the boundary condition from the experimental results. The stress-strain diagram obtained from the test performed by the previous researchers [27] for this material, provides the material properties required for the FEA. Beremin model parameters are calculated using strain correction as proposed by the modified Beremin model, local criterion using the distribution of particle fracture stress, following exponential dependence of eligible microcracks on  $\epsilon_p$  (plastic strain) and under influence of plastic strain on microcrack density. The Weibull modulus ( $m$ ) and Weibull scale parameter ( $\sigma_u$ ) are calibrated by Monte Carlo simulation for temperatures -100°C, -110°C, -120°C, -130°C, -140°C from the experimental results as explained in the previous work [24]. Then  $C_{m,n}$  another Beremin parameter is also calibrated for the above-mentioned temperatures as described in the previous work of the author [28]. Once the  $C_{m,n}$  is calculated fracture toughness can be predicted for different temperatures from the above-mentioned models for different probability of failures. The predicted fracture toughness is compared with the experimental values.

In this work, the entire focus is being made on the brittle failure nature of German based reactor pressure vessel material (20MnMoNi 55 steel) at the lower self of DBT region, which is a very important study as far the safety of reactor pressure vessel is concerned. In recent years study on this material dealing with specific topics is not performed. Moreover, the application of Monte Carlo simulation to reduce the burden of performing a huge number of fracture experiments is overcome by this procedure. The author proves the success in the application of the statistical model by matching it with the experimental results in his previous work [29]. In the present work, the author utilizes the statistical model along with FEA to study the effect of strain on brittle fracture through four different strain corrected brittle fracture models. In the end, the fracture toughness predicted from these models is compared with the established ASTM E1921 and master curve results which is a very challenging and interesting part of the work.

2. Material

The material studied is German steel, used in the reactor pressure vessel of Indian PHWR and designated as 20MnMoNi55. The material used in this investigation has received from Bhabha Atomic Research Centre, Mumbai, India. The steel was received in the form of a rectangular block. The specimens were made from this block to determine the fracture toughness of the selected steel using J-integral analysis and the master curve methodology, to understand the fracture behavior of the steel. The RPV material properties during operation are defined by their initial values, material type, chemical composition, and operating stressors, mainly operating temperature and neutron influence. The chemical composition of 20MnMoNi55 is shown in Table 1.

Name of element	C	Si	Mn	P	S	Al	Ni	Mo	Cr	Nb
Percentage composition (in weight)	0.20	0.24	1.38	0.011	0.005	0.068	0.52	0.30	0.06	0.032

Table 1.  
Chemical composition of 20MnMoNi55.

### 3. Methods

#### 3.1 Calculation of reference temperature ( $T_0$ ) and master curve analysis

Brittle fracture probability according to Wallin [1–3], is defined as  $P_f$  for a specimen having fracture toughness  $K_{JC}$  in the transition region is described by a three-parameter Weibull model as shown by.

$$P_f = 1 - \exp \left[ - \left( \frac{K_{JC} - K_{\min}}{K_0 - K_{\min}} \right)^4 \right] \quad (1)$$

where,

$$K_{JC} = \sqrt{\frac{J_c \cdot E}{(1 - \nu^2)}} \quad (2)$$

Scale parameter  $K_0$  which dependent on the test temperature and specimen thickness, and  $K_{\min}$  is equal to 20 MPa $\sqrt{m}$  [29].

For single-temperature evaluation, the estimation of the scale parameter  $K_0$ , is performed according to Eq. (4).

$$K_0 = \left[ \sum_{i=1}^N \frac{(K_{JC(i)} - K_{\min})^4}{N} \right]^{1/4} + K_{\min} \quad (3)$$

$$K_{JC(\text{median})} = K_{\min} + (K_0 - K_{\min})(\ln 2)^{1/4} \quad (4)$$

Here,  $T_0$  is the temperature at which the value of  $K_{JC(\text{median})}$  is 100 MPa $\sqrt{m}$  and is known as the reference temperature.  $T_0$  can be calculated from.

$$T_0 = T_{\text{test}} - \frac{1}{0.019} \ln \left[ \frac{K_{JC(\text{median})} - 30}{70} \right] \quad (5)$$

#### 3.2 Modified Beremin model

According to the Beremin model [21], the probability of failure is given as,

$$P_f = 1 - \exp \left( - \left( \frac{\sigma_w}{\sigma_u} \right)^m \right) \quad (6)$$

$$\sigma_w = \sqrt[m]{\left( \sum_{j=1}^n \sigma_1^j \right)^m \frac{V_j}{V_0}} \quad (7)$$

$n$  is the number of volumes  $V_j$ , or elements in a FEM calculation, and  $\sigma_1^j$  the maximal principal stress of the element  $j$  and  $V_j/V_0$  is just a scaling based on the assumption that the probability scales with the volume.  $V_0$  is the reference volume which is normally taken as a cubic volume containing about 8 grains i.e.,  $50 \times 50 \times 50 \mu\text{m}$ .

The classical model described above is applicable where plastic strain is negligible or zero for perfectly brittle materials but for ferritic steels where an appreciable amount of plastic strain is observed in the crack tip area this formula cannot capture the failure mechanism perfectly. To impose plastic strain effect on the failure mechanism a correction formulation has been introduced by Beremin [21].



$$\sigma_w = \sqrt[m]{\sum_j \left(\sigma_1^j\right)^m \frac{V_j}{V_0} \exp\left(-\frac{m\varepsilon_1^j}{2}\right)} \quad (8)$$

$\varepsilon_1^j$  is the strain in the direction of the maximum principal stress  $\sigma_1^j$ .

Throughout the paper, the Weibull stress is calculated according to Eq. (8).

### 3.3 Local approach to cleavage fracture incorporating plastic strain effects

This methodology is derived from the work done by Wallin and Laukkanen [30] which is based on the strain effect near the crack tip field. Here the Weibull stress is modified by taking into account a particular volume  $\delta V$  in the fracture process zone is subjected to a principal stress  $\sigma_1$  and associated with a plastic strain ( $\varepsilon_p$ ). In this mode micro-crack formed by the cracking of brittle particles only participate in the fracture process. It is assumed by Ruggieri and Dodds [30] that a fraction represented by  $\psi_C$  of the total number of brittle particles present in FPZ is responsible for nucleating the micro cracks which propagate unstably. This fraction  $\psi_C$  is a function of plastic strain but does not depend on microcracks. Based on the weakest link concept limiting distribution for the cleavage fracture stress can be expressed as.

$$P_f(\sigma_1, \varepsilon_p) = 1 - \exp \left[ -\frac{1}{v_0} \int_{\Omega} \psi_c \sigma_1^m d\Omega \right]^{1/m} \quad (9)$$

$V_0$  represents a reference volume conventionally taken as a unit volume.

$\Omega$  is the volume of the near-tip fracture process zone where  $\sigma_1 \geq \lambda \sigma_y$ .  $\lambda = 2$  [30, 31] is normally taken as twice of yield stress for the material.

Now  $\psi_C$  is calculated as follows.

$$\psi_c = 1 - \exp \left[ -\left(\frac{L}{L_N}\right)^3 \left(\frac{\sigma_{pf}}{\sigma_{prs}}\right)^{\alpha_p} \right] \quad (10)$$

$L$  represents the particle size;  $L_N$  a reference particle size;  $\sigma_{prs}$  is the particle reference fracture stress;  $\alpha_p$  denotes the Weibull modulus shape parameter of particle distribution; and  $\sigma_{pf}$  represents the characteristics of fracture stress.

$$\sigma_{pf} = \sqrt{1.3\sigma_1\varepsilon_p E} \quad (11)$$

where  $\sigma_1$  represents maximum principal stress,  $\varepsilon_p$  denotes the Maximum plastic strain of those particles whose  $\sigma_1$  is calculated in the fracture process zone (where  $\sigma_1 = 2 \sigma_y$ ) and  $E$  represents the Youngs Modulus of the particle at different temperatures. Now as assumed by Rugeirri et al. [25] the size of a fracture particle takes the size of a Griffith-like micro-crack of the same size the probability distribution of the fracture stress with increase loading for a cracked solid is given by the following equation.

$$P_f(\sigma_1, \varepsilon_p) = 1 - \exp \left[ -\frac{1}{v_0} \int_{\Omega} \left\{ 1 - \exp \left[ -\left(\frac{\sigma_{pf}}{\sigma_{prs}}\right)^m \right] \right\} \left(\frac{\sigma_1}{\sigma_u}\right) d\Omega \right]^{1/m} \quad (12)$$

As  $\psi_c$  is independent of microcrack size so  $L/L_N$  is considered to be 1. Therefore,  $\sigma_W$  takes the form.

$$\sigma_W = \left[ \frac{1}{V_0} \int_{\Omega} \left\{ 1 - \exp \left[ - \left( \frac{\sigma_{pf}}{\sigma_{prs}} \right)^{\alpha_p} \right] \right\} \sigma_1^m d\Omega \right]^{1/m} \quad (13)$$

### 3.4 Exponential dependence of eligible micro-cracks on $\epsilon_p$

Bordet et al. [31] include plastic strain effects on cleavage fracture in terms of the probability of nucleating a carbide micro crack. The original model considered only freshly nucleated carbides to act as Griffith-like micro-cracks and have the eligibility to propagate unstably take part in the fracture process. But in our work, we considered a simplified model as considered by Bordet et al. [31] and adopt a Poisson distribution by introducing a parameter  $\lambda$  to define  $\psi_c$  given by the following equation.

$$\psi_c = 1 - \exp(\lambda \epsilon_p) \quad (14)$$

$\lambda$  is assumed as the average rate of fracture particles which becomes Griffith-like micro crack with small strain increment. The author has taken the strain increment inconsistency with the quasi-static process. Therefore, the probability of fracture and Weibull stress takes the following form.

$$P_f(\sigma_1, \epsilon_p) = 1 - \exp \left[ - \frac{1}{v_0} \int_{\Omega} \left\{ 1 - \exp(-\lambda \epsilon_p) \right\} \left( \frac{\sigma_1}{\sigma_u} \right) d\Omega \right]^{1/m} \quad (15)$$

$$\sigma_W = \left[ \frac{1}{V_0} \int_{\Omega} \left\{ 1 - \exp(-\lambda \epsilon_p) \right\} \sigma_1^m d\Omega \right]^{1/m} \quad (16)$$

### 3.5 Influence of plastic strain on microcrack density

Based upon the work of Brindley and Gurland [32–34] the direct effect of plastic strain on micro-cracking of ferritic steel at different temperatures alter the probability distribution in the FPZ as follows:

$$P_f(\sigma_1, \epsilon_p) = 1 - \exp \left[ - \frac{1}{v_0} \int_{\Omega} \epsilon_p^{\beta} \left( \frac{\sigma_1}{\sigma_u} \right)^m d\Omega \right] \quad (17)$$

and the Weibull Stress becomes.

$$\sigma_W = \left[ \frac{1}{V_0} \int_{\Omega} \epsilon_p^{\beta} \cdot \sigma_1^m d\Omega \right]^{1/m} \quad (18)$$

## 4. Test procedure

### 4.1 Fatigue pre-cracking

The fracture toughness tests in this investigation were planned on three-point bending (TPB) specimens in L-T orientation. Standard 1T TPB specimens were

machined following the guidelines of ASTM E 399-90. The designed dimensions of the specimens were; thickness (B) 25 mm and width (W) = 25 mm which is constant for all the specimen tested and machined notch length (aN) = 10 mm to produce different a/W ratio of 0.5. Fatigue pre-cracking of the TPB specimens was carried out at room temperature at constant  $\Delta K$  mode as described in ASTM standard E 647 on servo hydraulic INSTRON UTM (Universal Testing Machine) with 8800 controllers having 100 KN grip capacity using a commercial da/dN fatigue crack propagating software supplied by INSTRON Ltd. U.K. The crack lengths were measured by compliance technique using a COD gauge of 10 mm gauge length mounted on the load line of the specimen.

#### 4.2 Fracture test

The estimation of J-integral values of the fabricated specimens was carried out using an INSTRON UTM (Universal Testing Machine) with an 8800 controller with 100 KN grip capacity as described earlier. Tests were done at different temperatures ranging from  $-100^{\circ}\text{C}$  to  $-140^{\circ}\text{C}$ . The specimen used is a three-point Bending specimen. The nomenclature along with a picture of the specimen is shown in **Figure 1**.

The Instron FAST TRACK JIC Fracture Toughness Program was used to determine the value of the J integral. This program performs Fracture Toughness on metallic materials following the American Society for Testing and Materials (ASTM) Standard test method E813. The method is applied specifically to specimens that have notches or flaws that are sharpened with fatigue cracks. The loading rate was slow, and cracking caused by environmental factors was considered negligible.

#### 4.3 A result of the tensile test and $J_{1C}$ at different temperatures in the lower self of the DBT region

From the experimental stress-strain results performed at different temperatures for 20MnMoNi55 steel, a clear plastic zone is observed before failure as shown in **Figure 2** [35]. The same plastic strain effect is reflected in the TPB specimen also at the lower self of the DBT region. This provoked us to perform the required strain correction in computing Weibull Stress through different strain correction models as discussed above.

The results of  $K_{JC}$  values of TPB specimens at different temperatures are shown in **Figure 3**.

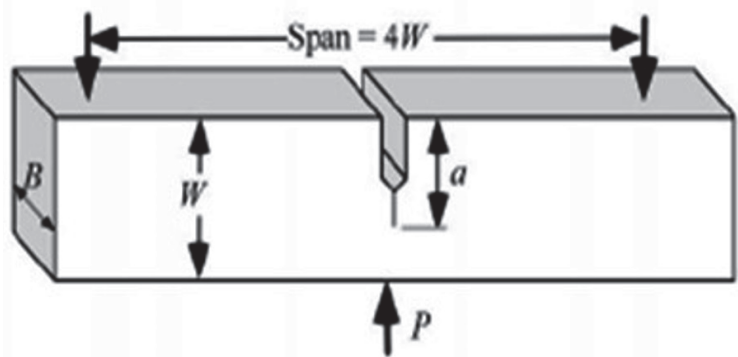


**Figure 1.**  
1T TPB specimen.



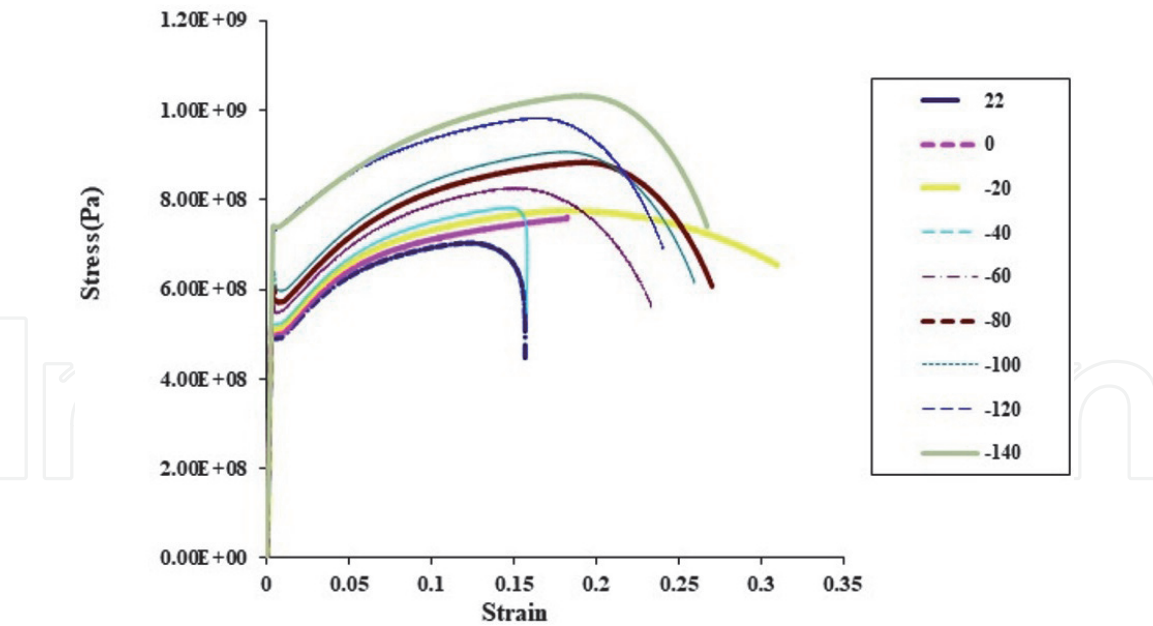


Figure 2. Stress-strain diagram of 20MnMoNi55 steel at different temperatures [27].

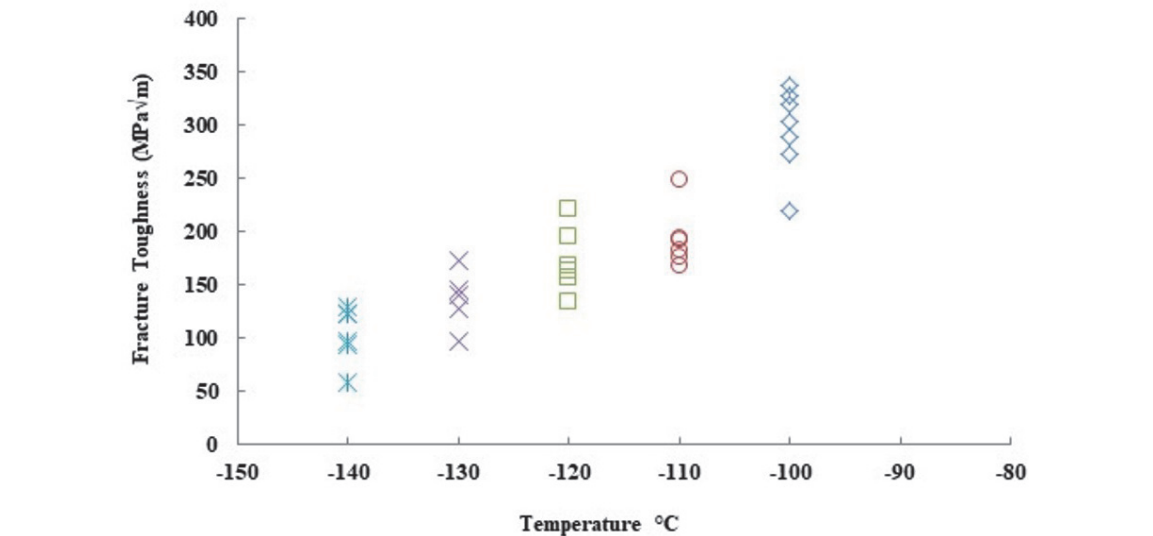
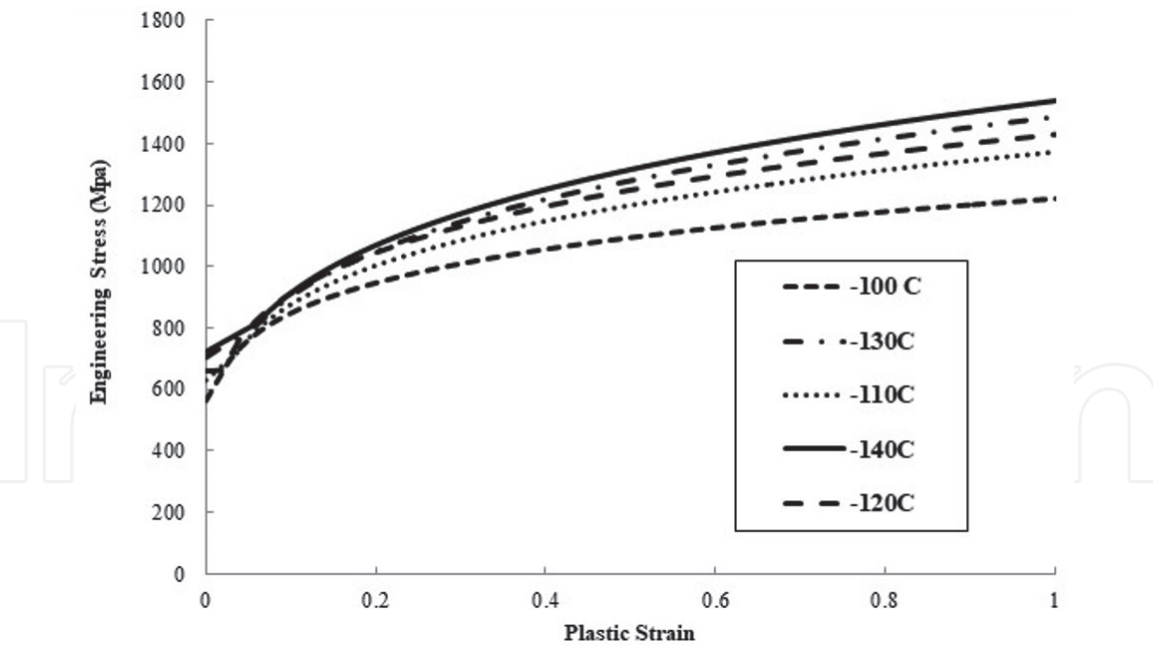


Figure 3.  $K_{IC}$  calculated from fracture toughness test at  $-110^{\circ}\text{C}$ .

4.4 Finite element analysis

Finite element analysis of all the fracture tests is performed using ABAQUS 6.13. The material constitutive properties are defined by Young’s modulus  $E$ , Poisson’s ratio  $\nu$ , and yield stress versus plastic strain obtained from tensile test data performed at different cryogenic temperatures [27]. **Figure 4** shows the stress versus plastic strain diagram at different temperatures and **Table 2** gives the yield stress and ultimate stress versus temperature for 20MnMoNi55 steel at different temperatures in the Brittle Dominated DBT region which is used as a material input parameter for elastoplastic finite element analysis. Isotropic elastic and isotropic hardening plastic material behavior are considered for the material used. 3-D finite element modeling is done for quarter TPB specimen at different temperatures to calculate the Weibull stress for the specimen and hence to calculate  $T_0$  from the Beremin model. The FE model has meshed with 8-node isoparametric hexahedral elements with 8 Gauss points taken for all calculations as referred by



**Figure 4.**  
*Engineering stress versus plastic strain for 20MnMoNi55 steel at different temperatures in the brittle dominated DBT region.*

Temperature (°C)	Yield strength (MPa)	Ultimate strength (MPa)
−100	593.43	760.49
−110	630.43	786.56
−120	667.06	813.66
−130	701.451	825.054
−140	723.47	856.84

**Table 2.**  
*Yield stress and ultimate stress versus temperature for 20MnMoNi55 steel at different temperatures in the brittle dominated DBT region.*

IAEA-TECDOC-1631 [36]. Reduced integration with full Newtonian non-linear analysis computation is carried out for all the specimens. In the region ahead of the crack tip the mesh was refined with an element volume of  $0.05 \times 0.05 \times 0.05 \text{ mm}^3$ . To facilitate the calculation of  $V_j$ , the element size is kept constant near the crack tip [36, 37]. Since a large strain is expected in the crack tip field, a finite strain (large deformation theory) method is used. As the crack extension during the experiment is found to be very small, the crack growth is not simulated in this FE analysis. **Figure 5** shows the boundary conditions and the mesh of the specimen. **Figure 6** shows the region where maximum principal stress exceeded twice the yield stress at that temperature. This region is known as the fracture process zone (FPZ). For such elements, the strain in the direction of the maximum principal stress is also calculated.

4.5 Validation of the FE model and material properties

**Figures 7–9** gives a comparison between experimental load versus load line displacement (LLD) of TPB specimen with FE simulated results from Abaqus 6.13 at the  $-100^\circ\text{C}$ ,  $-110^\circ\text{C}$  and  $-130^\circ\text{C}$  temperatures The FEA results show a close match with experimental results which validate the used FE model and material

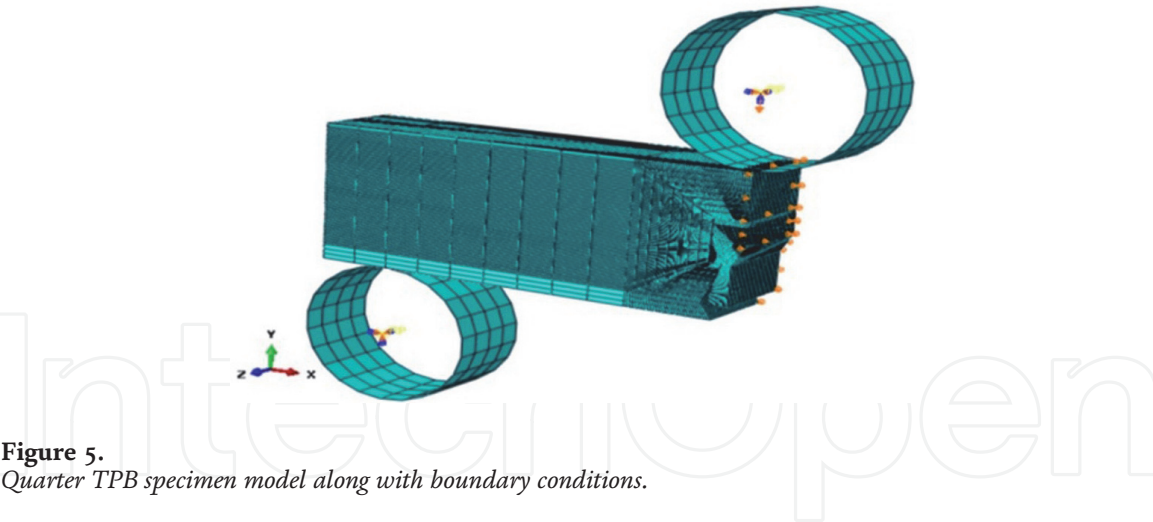


**Figure 5.**  
*Quarter TPB specimen model along with boundary conditions.*

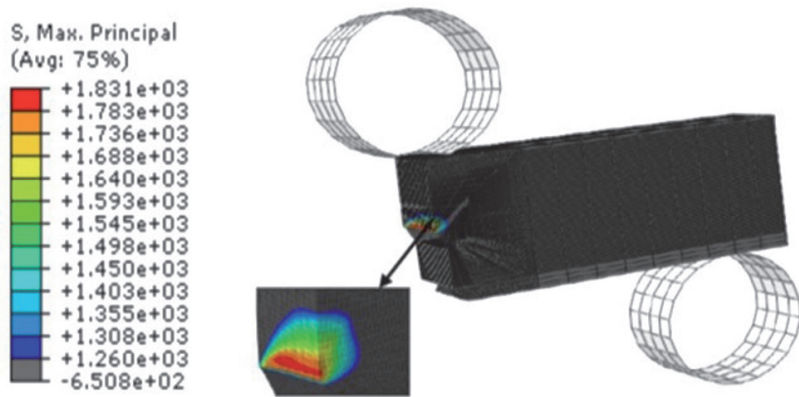


**Figure 6.**  
*Maximum principal stress (MPa) distribution in the fracture process zone.*

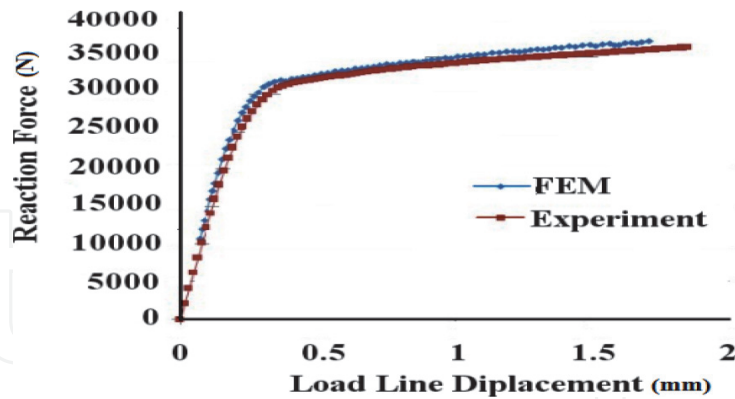


**Figure 7.**  
*Comparison of load vs. load line displacement (LLD)  $-100^{\circ}\text{C}$ .*

parameters. Now for each analysis, the Weibull stress at the failure point can be computed from the FE simulated results.

**4.6 Calculation of Weibull stress**

Now the maximum principal stress and corresponding strain in the direction of principal stress is known for each element in the fracture process zone, we calculate the Weibull Stress for each model using Eqs. (8), (13), (16), and (18).

The success of the Beremin model for predicting brittle fracture mainly depends on the accuracy of the values of the Beremin material parameters  $m$  and  $\sigma_u$ . The

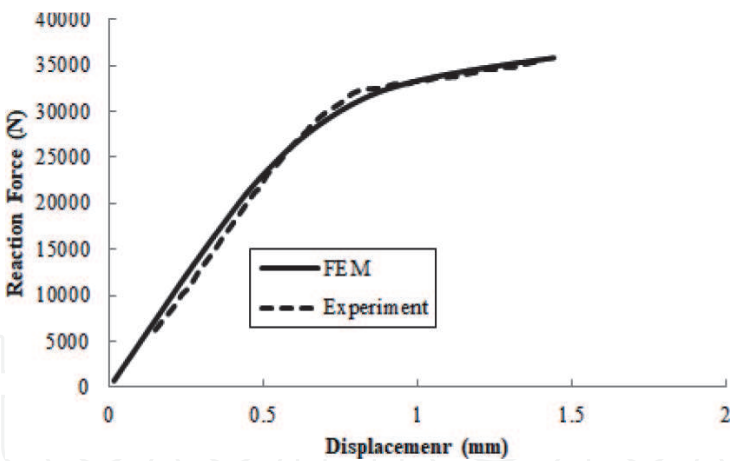


**Figure 8.**  
*Comparison of load vs. load line displacement (LLD)  $-110^{\circ}\text{C}$ .*

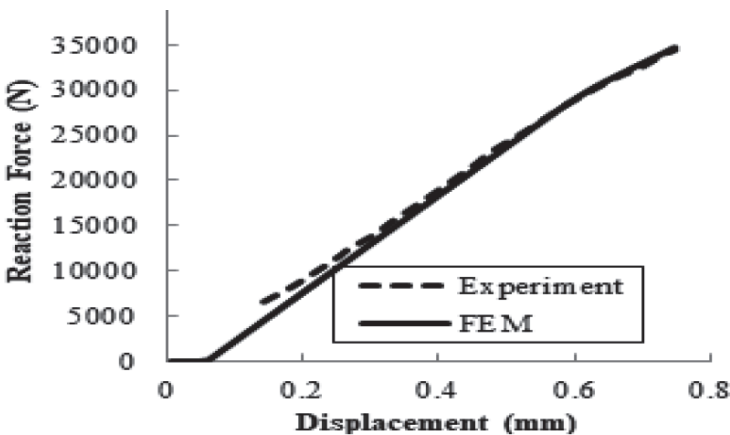


**Figure 9.**  
*Comparison of load vs. load line displacement (LLD)  $-130^{\circ}\text{C}$ .*

Beremin model describes the failure mechanism as an outcome of the distribution of the weakest sites in the statistical material. Hence any material parameters to represent the failure behavior should be determined from a large sample containing variation in candidatures as much as possible. With this in mind, the values of  $m$  and  $\sigma_u$  have been determined from the experimental fracture toughness tests at  $-100^{\circ}$ ,  $-110^{\circ}$ ,  $-130^{\circ}$  which is described as a direct calibration strategy. The process is described vividly for  $-110^{\circ}\text{C}$  by K. Bhattacharyya et al. calibration of beremin parameters for 20MnMoNi55 Steel and prediction of reference temperature ( $T_0$ ) for different thicknesses and  $a/W$  ratios [28]. But testing such a huge number of specimens are very expensive so the author used to develop a random number of data with the help of master curve and Monte Carlo simulation [24]. This process is called an indirect calibration strategy. The entire process is described by the author in their previous work [23], step-wise description only the Step 7 of Article No.4 the Weibull Stress is calculated for different models using Eqs. (8), (13), (16), and (18). The validation of the results simulated from Monte Carlo simulation with the experimental work is also validated by the author in their previous work [24].

#### 4.7 Calibration of $C_{m,n}$

$C_{m,n}$  an important parameter used for the determination of  $K_{JC}$  for different models has been calibrated for this material at different temperatures. The process of determination of  $C_{m,n}$  for our material is different from that as framed by

Beremin. The entire process is described step by step for  $-110^{\circ}\text{C}$  in the previous work done by the author [28]. A similar procedure is used for the determination of  $C_{m,n}$  for other temperatures. Once  $C_{m,n}$  is calibrated the value of fracture toughness for 5%, 63.2%, and 95% can be determined by Eqs. (6), (9), (12), (15), and (17). These fracture toughness values were then plotted with the experimentally determined master curve methodology as shown in **Figure 12**.

5. Results and discussions

The calibration of Weibull modulus “ $m$ ” using different models as described above is shown in **Figure 10** and the Weibull scale parameter is shown in **Figure 11**. It is observed that the value of Weibull modulus for the four different models almost coincides at  $-100^{\circ}\text{C}$  and  $-110^{\circ}\text{C}$  and as the temperature decreases to  $-120^{\circ}\text{C}$  to  $-140^{\circ}\text{C}$  the variation of in the value of Weibull modulus predicted from the different model is pronounced and it increases with decrease in temperature. As the material moves from the lower self of DBT region to purely cleavage fracture the effect of ductile stretch due to plasticity affect vanishes. As all the four models are functions of plastic strain therefore as it approaches purely brittle failure the strain component almost vanishes therefore prediction capability of the models to some extent becomes biased.

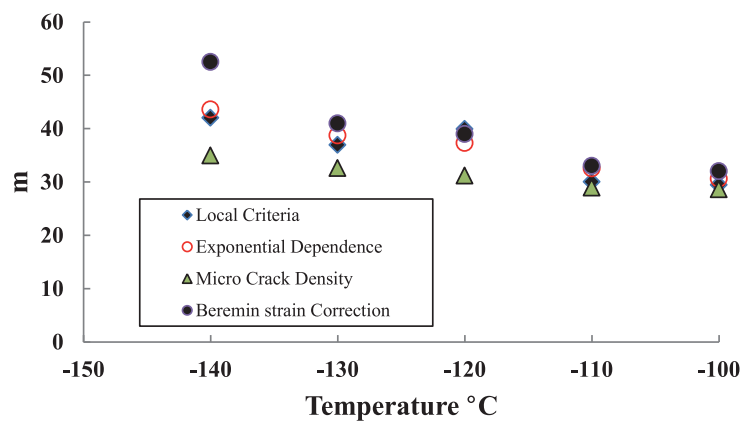


**Figure 10.** Variation of Weibull modulus “ $m$ ” for different temperatures using different strain correction model is shown.

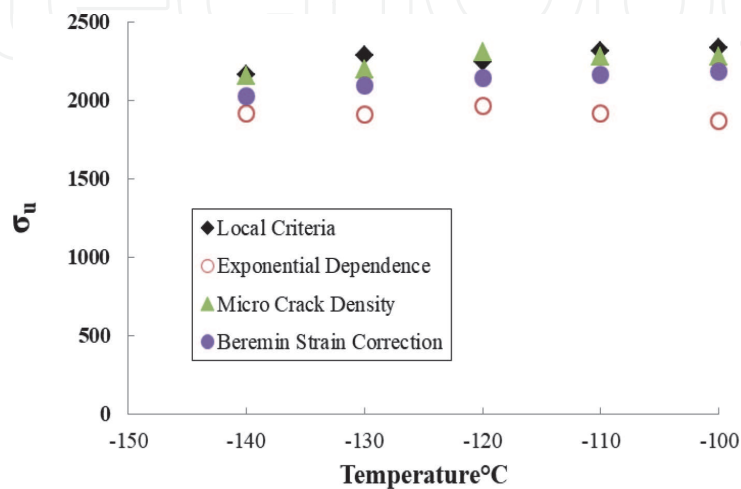


**Figure 11.** Variation of Weibull modulus scale parameter “ $\sigma_u$ ” for different temperatures using different strain correction model is shown.



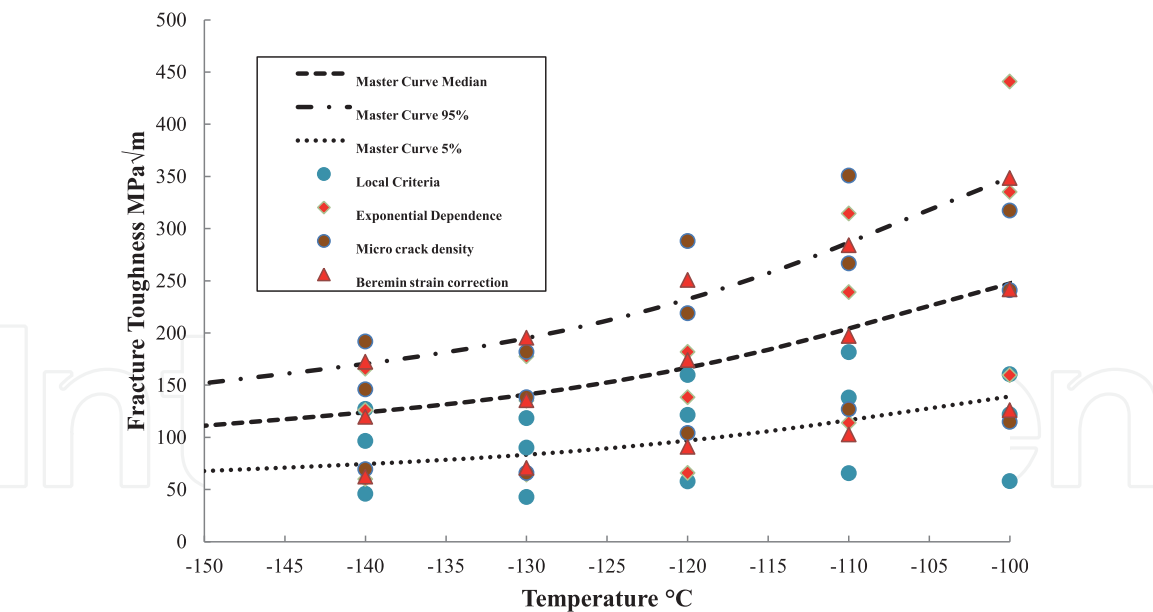


**Figure 12.**  
*Master curve determined from experimental results of  $-120^{\circ}\text{C}$  compared with the fracture toughness determined from various models.*

Weibull modulus “ $m$ ” and Weibull modulus scale parameter “ $\sigma_u$ ” is calculated from different models as explained, now once  $C_{m,n}$  is calculated at different temperatures, fracture toughness can be predicted for different probabilities of failure.

It is observed that the prediction capability Beremin strain correction model is much better in comparison to the other three models when validated with the experimental results as shown in **Figure 12**.

Though Claudio Ruggieri and his co-workers in their work [25] showed that fracture toughness predicted from local criteria matches well with the experimental results for A515 Gr 65 pressure vessel steel but the results obtained in this study appear to be contradictory with their work for the material 20MnMoNi55 steel.

Our study is focussed on the lower self of DBT region starting from  $-100^{\circ}\text{C}$  to  $-140^{\circ}\text{C}$  where a very small amount of ductile stretch is observed before failure but their work is focussed at  $-20^{\circ}\text{C}$  where a huge amount of ductile stretch is observed before cleavage failure for our material. This could be one reason for the deviation of the results with them.

The main aim of this work is to establish the strain affect in the brittle failure-dominated portion of the DBT region, which is observed in the form of ductile stretch in experimental results.

## 6. Conclusion

1. With the help of finite element analysis, we have a better outlook in fracture process zone and we can bridge the gap between macroscopic observations (like J-integral and fracture toughness) with micro-cracks developed in the fracture process zone.
2. The effect of strain is established in the brittle failure dominated portion of DBT region through different strain correction model.
3. Utilization of statistical model (Monte Carlo simulation) proves to be very useful to reduce the huge cost of performing a large number of experiments at the cryogenic conditions.

4. The values of the Weibull modulus “ $m$ ” and Weibull modulus scale parameter “ $\sigma_u$ ” are calibrated through different brittle fracture models for different temperatures in the brittle failure dominated portion of DBT region for the concerned material.
5.  $C_{m,n}$  another important parameter is also calculated for different temperatures for the concerned material.
6. With the help of Weibull modulus “ $m$ ” and Weibull modulus scale parameter “ $\sigma_u$ ” and  $C_{m,n}$  the fracture toughness is predicted for different probabilities of failure.
7. The probabilities of failure are then compared with experimentally obtained results.
8. It is observed that the prediction capability Beremin strain correction model is much better in comparison to the other three models when validated with the experimental results.

Whenever fracture mechanics is used from specimen level to component level there is a constrain loss which affects the results. This causes a great lacuna in the application of fracture mechanics to the real engineering problems. This study to some extent put a step forward in overcoming the lacuna by using extensive finite element analysis and different brittle fracture models on specimen level and tried to predict the results in comparison with experimental counterpart. With the hope that in future application of fracture mechanics will not be limited to specimen level. This study will propel more research work in this field and the development of new models.


### Author details

Kushal Bhattacharyya

Department of Mechanical Engineering, Netaji Subhash Engineering College,  
Kolkata, India

\*Address all correspondence to: [bhattacharyyakushal3@gmail.com](mailto:bhattacharyyakushal3@gmail.com)

### IntechOpen

© 2021 The Author(s). Licensee IntechOpen. This chapter is distributed under the terms of the Creative Commons Attribution License (<http://creativecommons.org/licenses/by/3.0>), which permits unrestricted use, distribution, and reproduction in any medium, provided the original work is properly cited. 

## References

- [1] Wallin K. The scatter in KIC result. *Engineering Fracture Mechanics*. 1984; **19**:1085-1093
- [2] Wallin K. The master curve method: a new concept for brittle fracture. *International Journal of Materials and Product Technology*. 1999; **14**(2-4): 342-354
- [3] Wallin. K, Master Curve of ductile to brittle transition region fracture toughness round-robin data. The "EURO" Fracture toughness curve. VTT Report 1998. ISBN 951-38-5345-4
- [4] Bhattacharyya K et al. Study of constraint effect on reference temperature ( $T_0$ ) of reactor pressure vessel material (20MnMoNi55 Steel) in the ductile to brittle transition region. *Procedia Engineering*. 2014; **86**:264-271
- [5] Ruggieri C et al. Transferability of elastic-plastic fracture toughness using the Weibull stress approach: Significance of parameter calibration. *Engineering Fracture Mechanics*. 2000; **67**:101-117
- [6] Gao X. An engineering approach to assess constraint effects on cleavage fracture toughness. *Engineering Fracture Mechanics*. 2001; **68**:263-283
- [7] Wallin K. The size effect in  $K_{Ic}$  results. *Engineering Fracture Mechanics*. 1985; **22**(1):149-163
- [8] Smith JA. The effect of crack depth (a) and crack depth to width ratio (a/W) on the fracture toughness of A533-B steel. *Journal of Pressure Vessel Technology*. May 1994; **116**(2): 115-121
- [9] Dodds RH et al. A framework to correlate a/W ratio effects on elastic-plastic fracture toughness ( $J_c$ ) *International Journal of Fracture*. 1991; **48**:1-22
- [10] Minnebo P. Constraint-Based Master Curve Analysis of a Nuclear Reactor Pressure Vessel Steel Results from an Experimental Program Carried Out within the IAEA CRP-8 Project. EUR 24092 EN-2009
- [11] Gupta M et al. A review of T-stress and its effects in fracture mechanics. *Engineering Fracture Mechanics*. Jan 2015; **134**:218-241. DOI: 10.1016/j.engfracmech.2014.10.013
- [12] Ayatollahi MR et al. Determination of  $T$  -stress from finite element analysis for mode I and mixed-mode I/II loading. *International Journal of Fracture*. 1998; **91**:283-298
- [13] Castro JTP et al. Comparing Improved Plastic Zone Estimates Considering Corrections based on T-Stress and a Complete Stress Fields. *Proceedings of "First IJFatigue & FFEMS Joint Workshop" Forni di Sopra (UD), Italy; 2011. pp. 58-65*
- [14] Wallin K. Quantifying Tstress controlled constraint by the master curve transition temperature  $T_0$ . *Engineering Fracture Mechanics*. 2001; **68**:303-328
- [15] Henry BS. The stress triaxiality constraint and the Q-value as a ductile fracture parameter. *Engineering Fracture Mechanics*. 1997; **57**(4):375-390
- [16] Moattari M. Modification of fracture toughness master curve considering the crack-tip Q-constraint. *Theoretical and Applied Fracture Mechanics*. Aug 2017; **90**:43-52. DOI: 10.1016/ j.tafmec.2017. 02.012
- [17] Cravero S. A Two-Parameter Framework to Describe Effects of Constraint Loss on Cleavage Fracture and Implications for Failure Assessments of Cracked Components J.

of the Braz. Soc. of Mech. Sci. & Eng. Apr 2019;**141**:021401-7.

[18] Graba M. The influence of material properties and crack length on the  $Q$ -stress value near the crack tip for elastic-plastic materials for centrally cracked plate in tension. Journal of Theoretical and Applied Mechanics. 2012;**50**(1):23-46

[19] Bhowmik S et al. Evaluation, and effect of loss of constraint on a master curve reference temperature of 20MnMoNi55 steel. Engineering Fracture Mechanics. 2015;**136**:142-157

[20] Bhattacharyya K et al. Modelling the constraint effect on reference temperature with finite element parameters for reactor pressure vessel material 20MnMoNi55 steel. Defence Science Journal. 2020;**70**(3):323-328. DOI: 10.14429/dsj.70.12886

[21] Beremin FM. A local criterion for cleavage fracture of a nuclear pressure vessel steel. Metallurgical and Materials Transactions A. 1983;**14A**:2277-2287

[22] Khalili A, Kromp K. Statistical properties of Weibull estimators. Journal of Materials Science. 1991;**26**: 6741-6752

[23] Bhattacharyya K et al. Variation of Beremin model parameters with temperature by Monte Carlo simulation. Journal of Pressure Vessel Technology. 2019;**141**:021401. DOI: 10.1115/1.4042121

[24] Ruggieri C, Dodds RH Jr. An engineering methodology for constraint corrections of elastic-plastic fracture toughness—Part I: A review on probabilistic models and exploration of plastic strain effects. Engineering Fracture Mechanics. 2015;**134**:368-390. DOI: 10.1016/j.engfracmech.2014.12.015

[25] Ruggieri C, Savioli RG, Dodds Jr RH. An engineering methodology for

constraint corrections of elastic-plastic fracture toughness—Part II: Effects of specimen geometry and plastic strain on cleavage fracture predictions. Engineering Fracture Mechanics. 2015; **146**:185-209. DOI: 10.1016/j.engfracmech.2015.06.087

[26] Ruggieri C, Dodds RH Jr. A local approach to cleavage fracture modeling: An overview of progress and challenges for engineering applications. Engineering Fracture Mechanics. Jan 2018;**187**:381-403. DOI: 10.1016/j.engfracmech.2017.12.021

[27] Ruggieri C. A modified local approach including plastic strain effects to predict cleavage fracture toughness from subsize precracked charpy specimens. Theoretical and Applied Fracture Mechanics. Feb 2020;**105**: 102421. DOI: 10.1016/j.tafmec.2019.102421

[28] Bhattacharyya K et al. Calibration of Beremin parameters for 20MnMoNi55 steel and prediction of reference temperature ( $T_0$ ) for different thicknesses and  $a/W$  ratios. Ratios Journal of Failure Analysis and Prevention. 2018;**18**:1534–1547. DOI: 10.1007/s11668-018-0549-7

[29] Bhattacharyya K, Acharyya S. Validation of Monte Carlo simulation technique for calibration of cleavage fracture model parameters, with the calibrated values from experimental results for reactor pressure vessel material 20MnMoNi55 steel in the lower self of ductile-to-brittle transition region. Journal of Pressure Vessel Technology. Dec 2021;**143**: 021401-1 to 021401-7. DOI: 10.1115/1.4051021

[30] Wallin K, Laukkanen A. New developments of the Wallin, Saario, Törrönen cleavage fracture model. Engineering Fracture Mechanics. 2008; **75**:3367-3377

- [31] Bordet SR, Karstensen AD, Knowles DM, Wiesner CS. A new statistical local criterion for cleavage fracture in steel. Part I: Model presentation. *Engineering Fracture Mechanics*. 2005;**72**:435-452
- [32] Brindley BJ. The effect of dynamic strain-aging on the ductile fracture process in mild steel. *Acta Metallurgica*. 1970;**18**:325-329
- [33] Lindley TC, Oates G, Richards CE. A critical appraisal of carbide cracking mechanism in ferritic/carbide aggregates. *Acta Metallurgica*. 1970;**18**: 1127-1136
- [34] Gurland J. Observations on the fracture of cementite particles in a spheroidized 1.05% C steel deformed at room temperature. *Acta Metallurgica*. 1972;**20**:735-741
- [35] Bhowmik S et al. Application and comparative study of master curve methodology for fracture toughness characterization of 20MnMoNi55 steel. *Materials and Design*. 2012;**39**:309-317
- [36] International Atomic Energy Agency. Master Curve Approach to Monitor Fracture Toughness of Reactor Pressure Vessels in Nuclear Power Plant, IAEA-TECDOC-1631, Vienna; 2009b
- [37] Tiwari A, Avinash G, Sunil S, Singh RN, Per Stahle Chattopadhyay J, et al. "Determination of Reference Transition Temperature of In-RAFMS in Ductile Brittle Transition Regime Using Numerically Corrected Master Curve Approach," *Engineering Fracture Mechanics*. 2015;**142**:79-92